Anal. Bioanal. Electrochem., Vol. 17, No. 2, 2025, 190-203
https://www.doi.org/10.22034/abec.2025.721576

Analytical & Bioanalytical Electrochemistry

www.abechem.com

Full Paper

Modified Carbon Paste Electrode Using MIL-101 (Fe) Metal-Organic Framework and Ionic Liquid for Ferrocene-Mediated Voltammetric Determination of Glutathione

Ali Rezaiezaded,[1] and Afsaneh Hajializade[2,*]

[1]*Department of Biological Science, Sirjan Branch, Islamic Azad University, Sirjan, Iran*
[2]*Department of Natural Resources, Sirjan Branch, Islamic Azad University, Sirjan, Iran*

*Corresponding Author, Tel.: +98-9132458862
E-Mail: a.hajializadeh@yahoo.com

Received: 11 October 2024 / Received in revised form: 20 February 2025 / Accepted: 23 February 2025 / Published online: 28 February 2025

Abstract- This study presents a novel electrochemical sensing technique for the quantitative analysis of glutathione levels, a crucial biomolecule linked to various medical conditions such as diabetes, Parkinson's disease, and cancer. The increasing demand for simple, rapid, and cost-effective assays in clinical diagnostics drives the need for innovative solutions. We synthesized the metal-organic framework (MOF) MIL-101(Fe) via a solvothermal method and characterized using Fourier-transform infrared (FT-IR) spectroscopy, X-ray diffraction (XRD), field-emission scanning electron microscopy (FESEM), and energy dispersive x-ray spectroscopy (EDX). Then, a modified carbon paste electrode using MIL-101 (Fe) MOF and ionic liquid (IL) for ferrocene (FC)-mediated electrochemical determination of glutathione was prepared (MIL-101 (Fe) MOF/FC/ILCPE). The electrochemical performance of the designed electrode was assessed through cyclic voltammetry (CV), linear sweep voltammetry (LSV), chronoamperometry, and differential pulse voltammetry (DPV). Based on the CV investigations, the as-prepared MIL-101 (Fe) MOF/FC/ILCPE demonstrated good electrocatalytic performance towards the oxidation of glutathione. The developed sensor demonstrated a broad linear dynamic range of 0.5–385.0 µM for glutathione detection. The limit of detection (LOD) was calculated as 0.15 µM. Practical applications were validated through the analysis of human urine and hemolyzed erythrocyte samples, showing exceptional effectiveness in glutathione detection. This electrochemical sensor exhibits significant potential for clinical applications in monitoring glutathione levels.

Keywords- Electrochemical techniques; Carbon paste electrode; Glutathione; Ionic liquids; MIL-101 (Fe) metal-organic framework; Ferrocene

1. INTRODUCTION

The biological thiols, such as glutathione, cysteine, and homocysteine, play vital roles in the human body and other living organisms. These compounds have special properties due to the presence of thiol groups (-SH) in their structure and are known as antioxidants and important agents in cellular metabolism. The quantification of glutathione (GSH) is vital due to its role as an antioxidant in managing oxidative stress within cells. GSH acts as a primary protective agent against oxidative damage, and its levels are indicative of cellular health and various pathological conditions in eukaryotic organisms. The ratio of GSH to its oxidized form, GSSG, is particularly informative; deviations from normal levels can signal oxidative stress, shedding light on cellular interactions with external factors during disease processes. Recent advancements have improved our capacity to monitor changes in thrombus formation, thereby enriching our understanding of numerous biological mechanisms [1]. Current methodologies for measuring GSH include high-throughput live cell imaging and liquid chromatography-tandem mass spectrometry (LC-MS/MS), both of which enhance the precision and reliability of GSH assessments. Moreover, reversible fluorescent probes are increasingly utilized for tracking GSH variations in living cells, providing critical insights for scientific research [1-3]. With ongoing research developments, electrochemical techniques are gaining traction for GSH analysis due to their heightened sensitivity, selectivity, and adaptability. These methods exploit the electroactive nature of GSH to enable direct measurement and quantification, which is essential for understanding its involvement in biological functions and disease mechanisms.

Among electrochemical techniques, voltammetry is a powerful electrochemical technique widely utilized for the analysis of compounds in the different fields such as medicine, environmental science, and food safety due to its high sensitivity and versatility. It enables both quantitative and qualitative analysis by measuring the current that flows in response to changes in the applied potential, allowing for the detection of compounds at very low concentrations [4-8]. Carbon paste electrodes (CPEs) have become widely adopted in electrochemical systems. Numerous enhancements have been made to improve CPE performance in GSH quantification through the incorporation of novel materials aimed at increasing sensitivity and selectivity [9]. Despite considerable evidence supporting the efficacy of modified CPEs for detecting GSH, challenges such as reproducibility and stability in practical applications persist. The integration of composite electrodes such as those incorporating multi-walled carbon nanotubes or graphene oxide has been shown to enhance electro-catalytic properties and stability, thus improving detection rates for GSH [10]. These modifications address issues like electrode passivation that can impede accurate GSH quantification [11]. Additionally, enhancements using ferrocene have been noted to significantly improve the electrochemical characteristics of CPEs by facilitating oxidation processes relevant to both glutathione and dopamine detection. The redox behavior of ferrocene is crucial as it undergoes reversible one-

electron oxidation and reduction necessary for effective charge transfer in electrochemical reactions [12-16].

The incorporation of iron-based MIL-101 metal-organic frameworks (MOFs) into CPEs has led to significant improvements in their electrochemical properties. MIL-101(Fe) enhances performance by providing easily accessible active redox sites along with increased surface area and conductivity that facilitate electron transfer during reactions. The abundance of active sites due to the large surface area of MIL-101(Fe) plays a crucial role in these processes [17]. The iron present within the MIL-101 structure is instrumental in enhancing charge storage and transfer during electrochemical reactions [18]. Furthermore, derivatives of MIL-101(Fe) exhibit remarkable electrocatalytic performance for oxygen reduction and evolution reactions that are essential for energy storage applications. However, challenges such as stability concerns and the need for optimization in synthesis methods may restrict the practical application of these materials [19].

The electrochemical performance of CPEs can be further improved by combining ionic liquids (ILs) with modifiers. This combination enhances stability, conductivity, and sensitivity, making these modified electrodes suitable for a range of analytical applications. ILs also serve effectively as epoxy hardeners in CPEs while acting as substitutes for plasticizers; thus, improving potential stability and conductivity [20]. CPEs that incorporate graphene nanocomposite alongside ILs demonstrate reduced overpotential and enhanced current response, enabling high-sensitivity detection of ciprofloxacin [21]. Additionally, integrating Ag nanoparticles with ILs has been shown to improve detection capabilities for hydrogen peroxide [22]. The electrocatalytic determination of GSH has already been reported in the various works such as 2,7-bis (ferrocenyl ethyl) fluoren-9-one modified CPE [23], multi-walled carbon nanotubes (MWCNTs)/azoferrocene derivative-modified CPE [24], iron (III) tetra-(N-methyl-4-pyridyl)-porphyrin/MWCNTs-modified basal plane pyrolytic graphite electrode (BPPGE) [25], TiO_2 nanoparticles/ferrocene carboxylic acid-modified CPE [26], cobalt phthalocyaninetetrasulfonate/Zn-Al layered double hydroxide (Zn-Al LDH)-modified glassy carbon electrode (GCE) [27], and etc. Although these reported electrochemical sensing platforms demonstrated efficient performance, the research on the development of electrochemical sensors for GSH determination should be continue to improve their practical application.

This work was performed with the aim of designing a new electrochemical sensing platform (MIL-101 (Fe) MOF/FC/ILCPE) for voltammetric determination of GSH. From cyclic voltammetry (CV) studies, it has been found that the MIL-101 (Fe) MOF/FC/ILCPE is a suitable platform for electrocatalytic oxidation of GSH. The MIL-101 (Fe) MOF/FC/ILCPE electrochemical sensor showed a linear detection range of 0.5 µM to 385.0 µM and a low limit of detection (LOD) of 0.15 µM. The designed sensing platform has been applied for GSH determination in the real samples.

2. EXPERIMENTAL SECTION

2.1. Reagents and chemicals

All the chemicals and reagents were used of analytical grade to ensure that our experimental results would be accurate and reliable. The purity levels of the chemicals were as follows: L-reduced glutathione (≥ 98%), sodium hydroxide (98%), iron(III) chloride hexahydrate (≥ 98%), terephthalic acid (99%), dimethylformamide (99.8%), and phosphoric acid (85%). We used all the reagents without further purification.

Electrochemical experiments were conducted using a conventional three-electrode system, controlled by an Autolab potentiostat/galvanostat (model PGSTAT 302N; Eco Chemie, the Netherlands) equipped with General Purpose Electrochemical System (GPES) software. The three-electrode setup comprised a working electrode, a reference electrode, and an auxiliary electrode. In this configuration, two distinct electrical loops are established: (1) a current loop between the working electrode and the auxiliary electrode, and (2) a measurement loop between the working electrode and the reference electrode. This setup ensures precise control over the electrochemical reactions and accurate measurement of the resulting signals.

The pH values of the solutions were determined using a digital pH meter (model 710, Metrohm), which provided reliable and reproducible measurements throughout the experiments.

For the electrochemical analyses, CV, chronoamperometry, and differential pulse voltammetry (DPV) techniques were employed. These measurements were carried out using the aforementioned Autolab PGSTAT 302N system, which is well-suited for such electrochemical studies due to its high sensitivity and stability. The GPES software facilitated data acquisition and analysis, enabling detailed characterization of the electrochemical behavior of the system under investigation.

2.2. Syntheses of MIL-101 (Fe) MOF

The synthesis of MIL-101 (Fe) MOF was performed based on the previous report by Gecgel et al. [28]. MIL-101 (Fe) MOF was synthesized by dissolving 2.48 mmol of $FeCl_3 \cdot 6H_2O$ (0.670 g) and 1.24 mmol of terephthalic acid (0.206 g) in 20 mL of dimethylformamide (DMF). The mixture was stirred for 20 minutes to achieve complete dissolution and homogeneity. Subsequently, the solution was transferred to a Teflon-lined autoclave and heated at 110 °C for 20 hours. After the reaction, the autoclave was allowed to cool to room temperature, and the resulting product was isolated by centrifugation. The product was then washed multiple times with DMF to remove any unreacted precursors or impurities. Finally, the purified MIL-101 (Fe) was dried overnight at 65 °C to yield the final product.

2.3. Preparation of modified electrochemical sensors (MIL-101 (Fe) MOF/FC/ILCPE)

The MIL-101 (Fe) MOF/FC/ILCPE was prepared using the following procedure: A mixture of 0.194 g graphite (98%), 0.004 g MIL-101 (Fe) MOF (2%), and 0.002 g ferrocene (FC, 1%) was thoroughly blended with suitable amounts of paraffin oil and IL in a mortar to form a homogeneous paste. These amounts of components were chosen to achieve the better sensitivity and response towards the oxidation of GSH. The resulting paste was then tightly packed into a glass holder (3.0 mm in diameter), and a copper rod was inserted to establish electrical contact. The surface of the modified electrode was smoothed using weighing paper to ensure a uniform and reproducible surface. For comparison, other CPEs were prepared following the same procedure.

2.4. Preparation of real sample

Hemolyzed erythrocytes and urine were used for real sample analysis by the standard addition method. These real samples were prepared according to previous reports procedures without any changes in them [29].

3. RESULTS AND DISCUSSION

3.1. Characterization of MIL-101 (Fe) MOF

The synthesized MIL-101 (Fe) MOF was characterized using a range of characterization techniques to confirm its structure, composition, and morphology. These analyses provided comprehensive evidence of the successful synthesis and properties of the material.

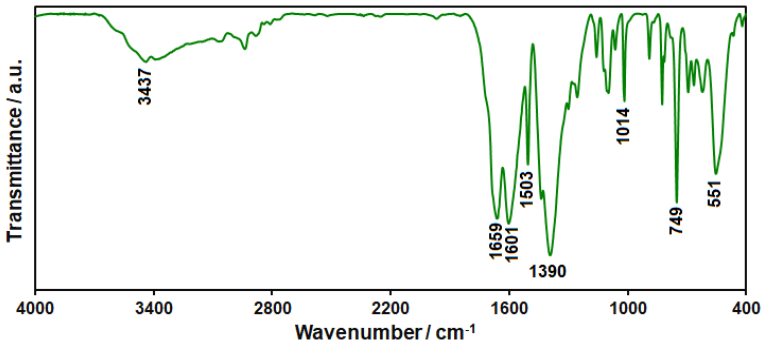

Figure 1. FT-IR spectrum of MIL-101 (Fe) MOF

FT-IR spectroscopy was used to identify the functional groups present in the MIL-101 (Fe) MOF (Figure 1). The spectrum displayed characteristic peaks at 749 cm^{-1}, 1014 cm^{-1}, 1390 cm^{-1}, 1503 cm^{-1}, 1601 cm^{-1}, and 1659 cm^{-1}, which are consistent with the typical features of MIL-101 (Fe) MOF [30]. The peaks at 1390 cm^{-1} and 1601 cm^{-1} correspond to the symmetric and asymmetric vibrations of carboxyl groups, respectively. The bands at 1503 cm^{-1} and 1659

cm^{-1} are attributed to the C=C stretching vibration of the benzene ring and the C=O stretching vibration in terephthalic acid, respectively. The peak at 749 cm^{-1} is associated with the bending vibration of C-H on the benzene ring, while the band at 551 cm^{-1} is assigned to the Fe-O vibration. Additionally, the broad absorption band at 3437 cm^{-1} is indicative of O-H stretching vibrations, likely due to adsorbed water or hydroxyl groups.

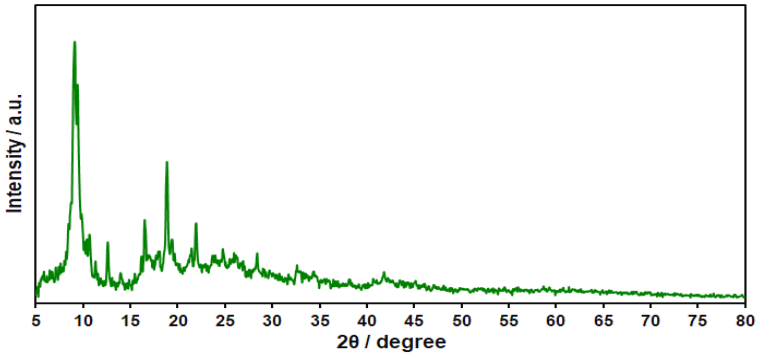

Figure 2. XRD pattern of MIL-101 (Fe) MOF

The crystalline structure and phase purity of the synthesized MIL-101 (Fe) MOF were confirmed by X-ray diffraction (XRD) analysis (Figure 2). The XRD pattern exhibited sharp and well-defined peaks, indicating high crystallinity. The observed pattern matched well with previously reported data [31-33], confirming the successful synthesis of MIL-101 (Fe) MOF.

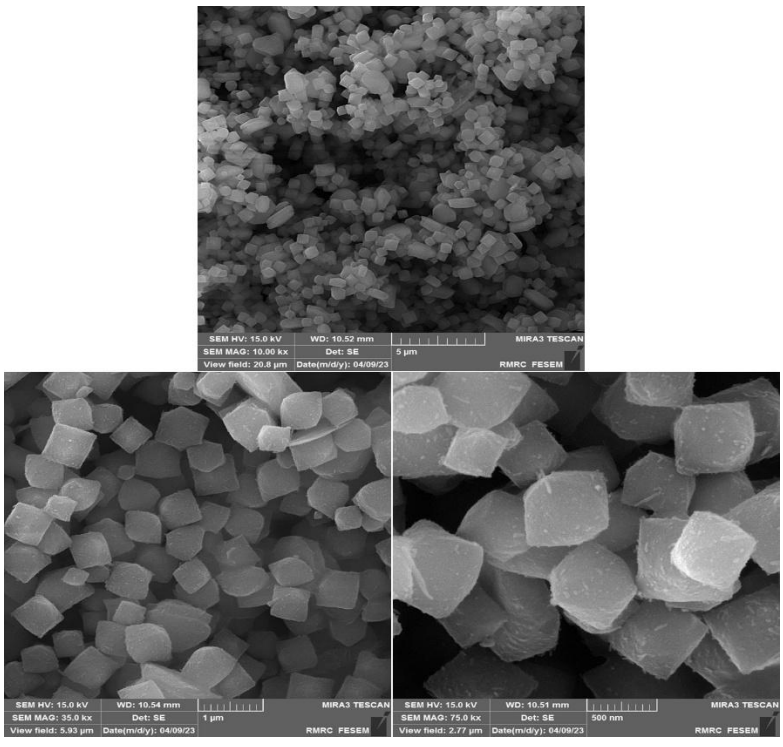

Figure 3. FE-SEM images of MIL-101 (Fe) MOF at various magnifications.

The morphology of the synthesized MIL-101 (Fe) MOF was investigated using field-emission scanning electron microscopy (FE-SEM). The FE-SEM images (Figure 3) revealed an octahedral morphology with an edge length of approximately 500 nm, consistent with the expected structure of MIL-101 (Fe) MOF.

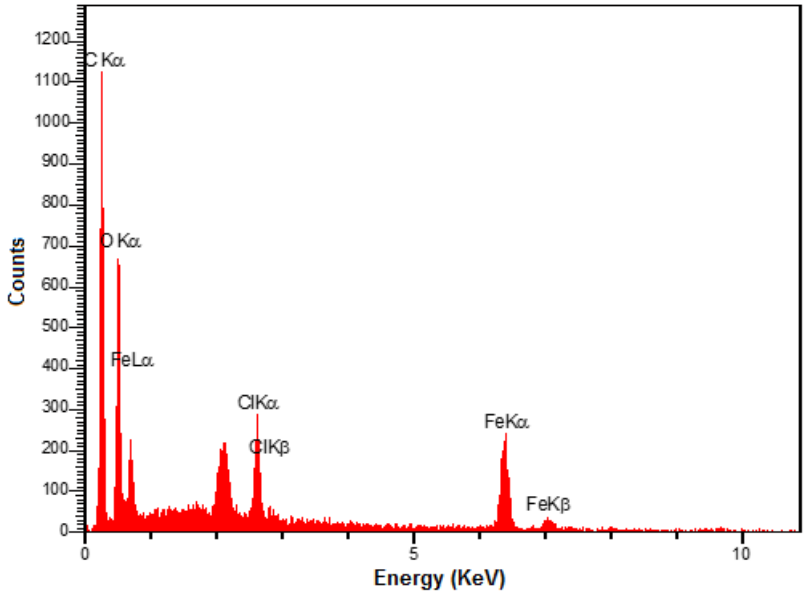

Figure 4. EDX spectrum of MIL-101 (Fe) MOF

Energy-dispersive X-ray spectroscopy (EDX) was used to analyze the elemental composition of the MIL-101 (Fe) MOF (Figure 4). The EDX spectrum confirmed the presence of Fe, C, O, and Cl elements, further supporting the successful formation of the MOF structure.

The combination of FT-IR, XRD, FE-SEM, and EDX analyses provides robust evidence for the successful synthesis and characterization of MIL-101 (Fe) MOF. These techniques collectively address the structural, compositional, and morphological aspects of the material, leaving no ambiguity about its formation. The results confirm that the synthesized MIL-101 (Fe) MOF exhibits the expected crystalline structure, functional groups, and elemental composition, making it suitable for further applications in sensing or catalysis.

3.2. pH optimization

pH dependence of the GSH oxidation at modified electrode shows mediated current maximum in neutral solution, so the medium of pH 7.0 was used for further studies.

3.3. GSH electrochemical behavior

The cyclic voltammograms obtained for MIL-101 (Fe) MOF/FC/ILCPE (in a phosphate buffer solution (pH 7.0) containing 100.0 µM GSH), FC/CPE (in a phosphate buffer solution (pH 7.0) containing 100.0 µM GSH), FC/CPE (in a phosphate buffer solution (pH 7.0) without

GSH) and an unmodified CPE (in a phosphate buffer solution (pH 7.0) containing 100.0 µM GSH) are shown in Figure 5. In the voltammogram d, GSH oxidation in bare CPE does not show any peaks. In the voltammogram c, the redox (anodic-cathodic) peak was observed for FC/CPE in the absence of GSH. In the voltammogram b, the anodic peak increased for FC/CPE in the presence of GSH, while the corresponding cathodic peak disappeared on the reverse scan. In voltammogram a, the anodic peak increased greatly for MIL-101 (Fe) MOF/FC/ILCPE in the presence of GSH, while the corresponding cathodic peak disappeared on the reverse scan.

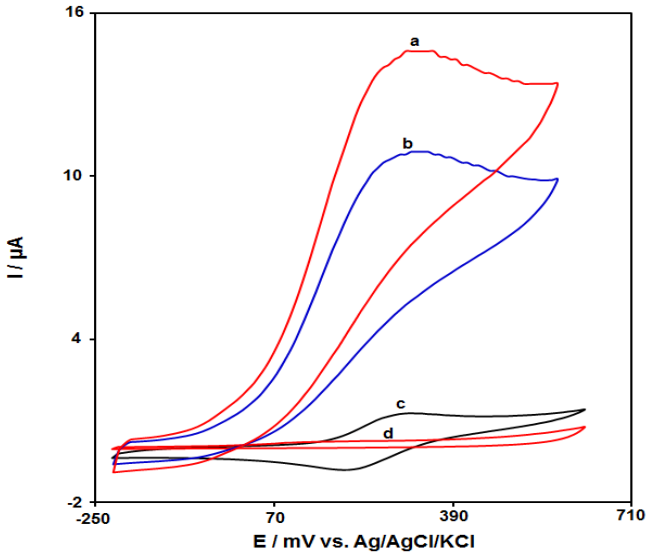

Figure 5. Cyclic voltammograms of a. MIL-101 (Fe) MOF/FC/ILCPE (in the presence of GSH, 100.0 µM); b) FC/CPE (in the presence of GSH, 100.0 µM); c) FC/CPE (in the absence of GSH) and d. CPE (in the presence of GSH, 100.0 µM) in 0.1 M phosphate buffer, pH 7.0) solution. (scan rate: 50 mV s^{-1})

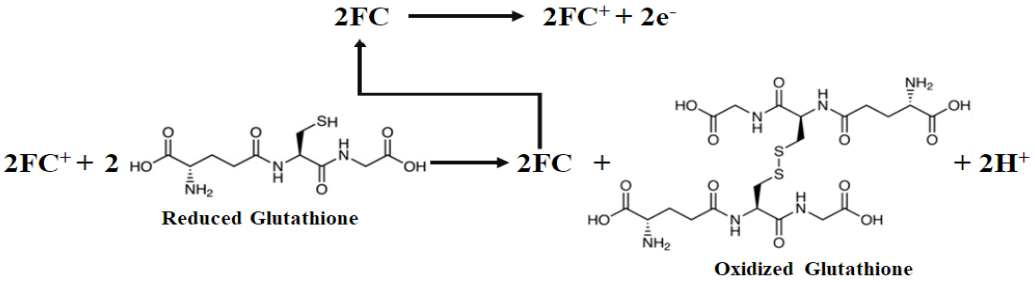

Scheme 1. Electrocatalytic oxidation mechanism of GSH at MIL-101 (Fe) MOF/FC/ILCPE

The reaction can be defined like this, which the electrogenerated FC^+ at the MIL-101 (Fe) MOF/FC/ILCPE surface catalyzes the oxidation of GSH. The FC^+ then undergoes a catalytic

reduction by GSH back to Fc, which can then be electrochemically reoxidized to produce an enhancement in the oxidation current. This mechanism is known as the kinetic mechanism of this electrocatalyzed reaction process (EC'). The proposed oxidation mechanism for GSH at MIL-101 (Fe) MOF/FC/ILCPE is depicted in Scheme 1. Effect of scan rate, CV was performed to check the effect of the scan rate on the peak current of GSH (50.0 µM, scan rate 5-100 mV/s) (Figure 6). To ascertain whether the electrochemical reactions are surface-assisted or diffusion-controlled, the relation between the signal intensity and scan rate was investigated. A linear plot between the peak current and scan rate shows a surface-controlled reaction, while linearity between the peak current and the square root of the scan rate shows a diffusion-controlled reaction. The oxidative peak current of GSH was plotted against the square root of the scan rate as shown in Figure 6. Thus, it has been found that Ip is linearly related to the square root of the potential scan rate ($v^{1/2}$), demonstrating GSH oxidation procedure has been difusion-controlled (Figure 6A). A plot of the scan rate-normalized current ($Ip/v^{1/2}$) vs. scan rate (Figure 6B) exhibits the characteristic shape typical of an EC´ process.

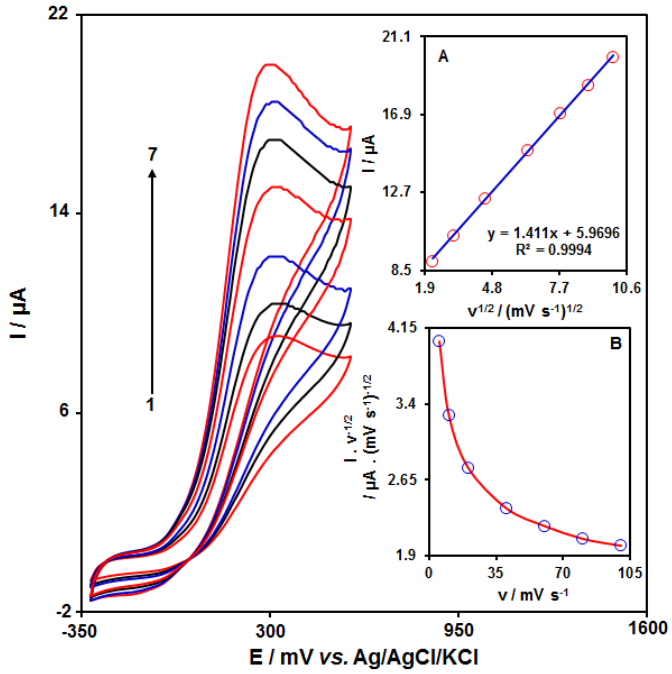

Figure 6. Cyclic voltammograms of 50.0 µM GSH at various scan rates: 5; 10; 20; 40; 60, 80 and 100 mV s^{-1} in 0.1 M buffer solution (pH 7.0); Plot of I_{pa} versus $v^{1/2}$ for the oxidation of GSH at the surface of MIL-101 (Fe) MOF/FC/ILCPE (Inset A) and Plot of $I_{pa}/v^{1/2}$ versus ν for the oxidation of GSH at the surface of MIL-101 (Fe) MOF/FC/ILCPE (Inset B)

To define the electron, transfer coefficient (α) between GSH and MIL-101 (Fe) MOF/FC/ILCPE, the Tafel diagram (E vs. log I) was drawn in the inset of Figure 7, using data from the ascending section of the voltammogram registered at 5 mVs^{-1} for 50.0 µM of GSH

(Figure 7). The calculated slope from the linear plot was equal to 0.2103. From the slope, the α value was estimated to be 0.72.

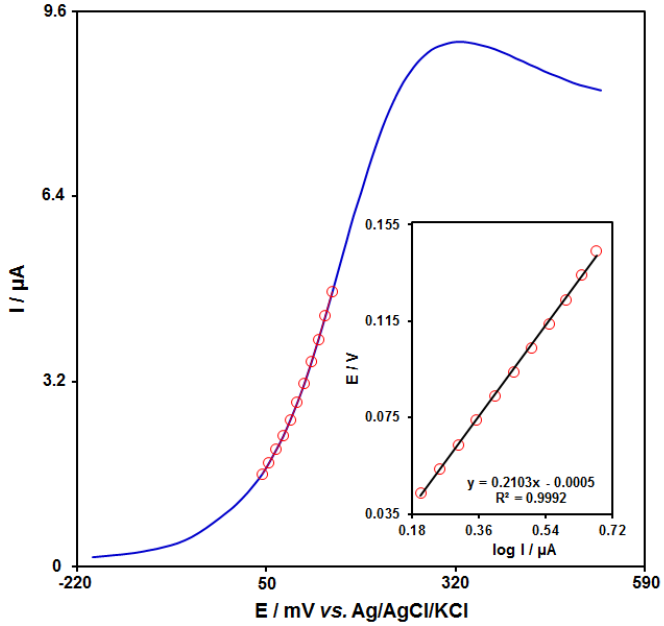

Figure 7. Tafel plot GSH (50.0 µM) at the surface of MIL-101 (Fe) MOF/FC/ILCPE in 0.1 M phosphate buffer (pH 7.0) at a scan rate of 5 mV s^{-1}

3.4. Chronoamperometry

The catalytic oxidation of GSH (0.1-1.0 mM) by MIL-101 (Fe) MOF/FC/ILCPE was studied by chronoamperometry. Chronoamperograms obtained at a potential step voltage of 410 mV are depicted in Figure 8. The mass transport limited current for the reaction of an electroactive material (GSH in this case) with a diffusion coefficient of D (cm^2 s^{-1}) and bulk concentration of C_b (mol cm^{-3}) is described by the Cottrell equation [34]:

$$I = nFAD^{1/2}C_b^{-1/2}t^{-1/2}$$

A plot of I versus $t^{-1/2}$ is found to be linear, the slope of which was used to obtain the value of D (Figure 8). The mean value of D was found to be 6.7×10^{-6} cm^2 s^{-1}.

3.5. Calibration curve and analytical parameters

To perform quantitative measurements, differential pulse voltammograms of MIL-101 (Fe) MOF/FC/ILCPE in detecting the various concentrations of GSH were recorded in the following conditions: step potential (0.01 V) and pulse amplitude (0.025 V). The calibration curve for the DPV peak current for GSH oxidation vs. GSH concentration (Figure 9) shows excellent linearity over a wide concentration range of 0.5 to 385.0 µM at pH 7.0 with a correlation coefficient of 0.9994 and can be expressed by the equation:

$$I_{pa}\,(\mu A) = 0.1235 C_{GSH}\,(\mu M) + 2.7554,\ R^2 = 0.9994$$

The LOD was estimated as 0.15 µM using the following equation: LOD = $3SD_{blank}$ (standard deviation of blank solution)/m (slope of the calibration curve). Modification of CPE by MIL-101 (Fe) MOF/FC/IL remarkably improves its performance towards the oxidation of GSH, thus, the quantitative limit of GSH in the solution is as low as possible. As much as 0.5 µM.

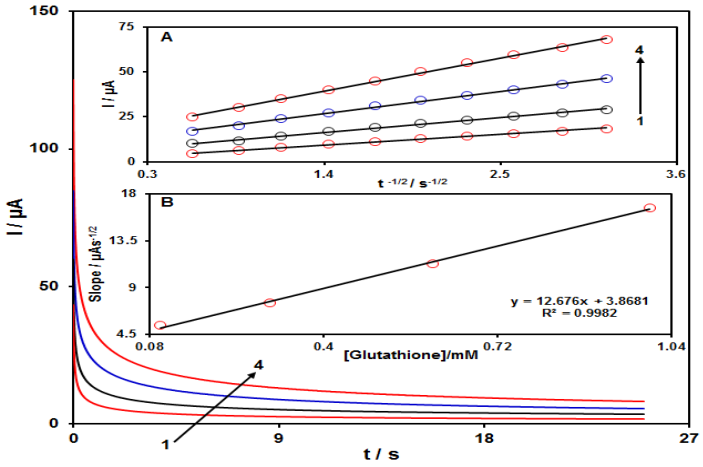

Figure 8. Chronoamperograms were gained at MIL-101 (Fe) MOF/FC/ILCPE in 0.1 M phosphate buffer (pH 7.0) at various levels of GSH concentration. 1 to 4 is corresponding to 0.1, 0.3, 0.6, and 1.0 mM of GSH. Insets: up - plots of I versus $t^{-1/2}$ achieved by chronoamperegrams 1–4; down-plot of the straight line slop vs. GSH concentrations

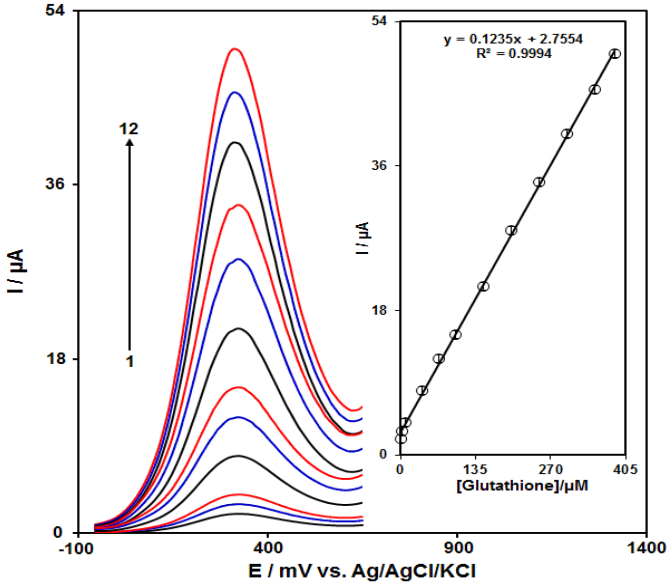

Figure 9. DPV responses of upon addition of increasing amounts of GSH (0.5, 3.0, 10.0, 40.0, 70.0, 100.0, 150.0, 200.0, 250.0, 300.0, 350.0, and 385.0 µM) in MIL-101 (Fe) MOF/FC/ILCPE (0.1 M phosphate buffer, pH 7.0) solution. Inset, Plot of I_{pa} versus concentration GSH at the surface of MIL-101 (Fe) MOF/FC/ILCPE

3.6. Determination of GSH in the presence of some ions

In order to perform the interference studies, determination of GSH in the presence of some ions was investigated at the surface of MIL-101 (Fe) MOF/FC/ILCPE. Based on the DPV measurements, it was observed that 400-fold Na^+, Mg^{2+}, Ca^{2+}, Cu^{2+}, NH_4^+, Cl^-, NO_3^-, and SO_4^{2-} did not show significant interference in GSH determination, and the peak currents were almost the same as the sample containing GSH without ion.

3.7. Spiked and real sample analysis

We also evaluated the practical feasibility of MIL-101 (Fe) MOF/FC/ILCPE for determining GSH in the real samples. A standard addition method was adopted in this experiment, and the corresponding results are listed in Table 1. The recovery was between 96.6% and 102.9% for GSH. In addition, the RSD of the real sample analysis varied from 1.6% to 3.6%. These results suggest that the electrochemical sensor is highly qualified for the determination of GSH in real applications.

Table 1. Analysis of GSH in the real specimens at the MIL-101 (Fe) MOF/FC/ILCPE (n = 5)

Sample	Spiked concentration (μM)	Measured Concentration (μM)	Recovery%	RSD%
Hemolyzed erythrocyte	0	4.8	-	-
	1.0	5.6	96.6	1.9
	2.0	6.6	102.9	3.6
	3.0	7.7	98.7	1.6
	4.0	8.9	101.1	2.9
Urine	0	-	-	-
	5.0	5.1	102.0	3.3
	7.5	7.4	98.7	1.8
	10.0	10.1	101.0	2.5
	12.5	12.4	99.2	2.8

4. CONCLUSION

The MIL-101 (Fe) MOF/FC/ILCPE was used as a sensing platform to detect GSH in human urine and hemolyzed erythrocyte. The electro-oxidation of GSH could be catalyzed by the Fc/Fc^+ couple as a mediator and had a higher electrochemical response due to the high surface area of MIL-101 (Fe) MOF and good conductivity of IL. The constructed electrode demonstrates a high sensitivity of 0.1235 μA/μM, a wide linear range of 0.5–385.0 μM. In addition, the designed sensing platform demonstrates good ability for GSH determination in the real samples.

Declarations of interest

The authors declare no conflict of interest in this reported work.

REFERENCES

[1] X. Li, Q. Wang, Q. Fang, J. Xu, B. Han, Y. Chen, W. Yao, S. Ye, and B. Wang, Mater. Adv. 4 (2023) 5003.

[2] T. Mathews, Quantitation of Glutathione and Oxidized Glutathione Ratios from Biological Matrices Using LC-MS/MS. Methods in Molecular Biology (MIMB, volume 2675).

[3] S. Nagabooshanam, A. Kumar, S. Ramamoorthy, N. Saravanan, and A. Sundaramurthy, Chemosphere 346 (2024) 140517.

[4] M.M. Foroughi, S. Jahani, and S. Rashidi, Microchem. J. 198 (2024) 110156.

[5] M.M. Foroughi, S. Jahani, S. Rashidi, O. Tayari, and M. Moradalizadeh, Mater. Chem. Phys. 315 (2024) 128893.

[6] S. Akbari, S. Jahani, M.M. Foroughi, and H.H. Nadiki, RSC Adv. 10 (2020) 38532.

[7] R. Rezaei, M.M. Foroughi, H. Beitollahi, and R. Alizadeh, Russ. J. Electrochem. 54 (2018) 860.

[8] H. Maaref, M.M. Foroughi, E. Sheikhhosseini, and M.R. Akhgar, Anal. Bioanal. Electrochem. 10 (2018) 1080.

[9] B. Ajdari, T. Madrakian, M.R.J. Sarvestani, and A. Afkhami, Talanta 283 (2025) 127174.

[10] S. Nagabooshanam, A. Kumar, S. Ramamoorthy, N. Saravanan, and A. Sundaramurthy, Chemosphere 346 (2024) 140517.

[11] S. Moris, L. Albornoz, J.A. Squella, and C. Barrientos, J. Electrochem. Soc. 171 (2024) 116502.

[12] N. Ukirade, S. Jagtap, and S. Rane, Hybrid Adv. 3 (2023) 100042.

[13] G. Roy, R. Gupta, S.R. Sahoo, S. Saha, D. Asthana, and P.C. Mondal, Coord. Chem. Rev. 473 (2022) 214816.

[14] J.L. Wang, T.Q. Chai, L.X. Chen, G.Y. Chen, H. Chen, and F.Q. Yang, Microchem. J. 199 (2024) 110207.

[15] Z.G. Khan, T.N. Agrawal, S.B. Bari, S.N. Nangare, and P.O. Patil, Spectrochim. Acta A Mol. Biomol. Spectrosc. 306 (2024) 123608.

[16] W. Li, Z. Xu, P. Li, X. Liu, C. Chen, Y. Zhang, M. Liu, and S. Yao, Microchim. Acta 191 (2024) 49.

[17] B. Akkinepally, G.D. Kumar, I.N. Reddy, H.J. Rao, P.C. Nagajyothi, A.A. Alothman, and J. Shim, Crystals 13 (2023) 1547.

[18] H. Mahajan, A.K. Shah, S. Kim, and S. Cho, ACS Omega 9 (2024) 24546.

[19] L. Hao, T. Yu, R. Guo, C. Liu, J. You, and H. Zhang, J. Energy Storage 90 (2024) 111828.

[20] A. Kopytowski, R. Świercz, D. Oniszczuk-Świercz, J. Zawora, J. Kuczak, and Ł. Żrodowski, Materials 16 (2023) 716.
[21] H. Shafiei, and S.K. Hassaninejad-Darzi, J. Electroanal. Chem. 935 (2023) 117321.
[22] A. Safavi, N. Maleki, and E. Farjami, Electroanalysis 21 (2009) 1533.
[23] J.B. Raoof, R. Ojani, and H. Karimi-Maleh, J. Appl. Electrochem. 39 (2009) 1169.
[24] M. Taei, H. Hadadzadeh, F. Hasanpour, G. Zahedi, and Z. Dehbanipour, IEEE Sens. J. 15 (2015) 4472.
[25] R.C. Luz, F.S. Damos, A.A. Tanaka, L.T. Kubota, and Y. Gushikem, Talanta 76 (2008) 1097.
[26] J.B. Raoof, R. Ojani, and M. Baghayeri, Sens. Actuators B: Chem. 143 (2009) 261.
[27] X. Wang, X. Chen, D.G. Evans, and W. Yang, Sens. Actuators B Chem. 160 (2011) 1444.
[28] C. Gecgel, U.B. Simsek, B. Gozmen, and M. Turabik, J. Iran. Chem. Soc. 16 (2019) 1735.
[29] H. Soltani, H. Beitollahi, A.H. Hatefi-Mehrjardi, S. Tajik, and M. Torkzadeh-Mahani, Anal. Bioanal. Electrochem. 6 (2014) 67.
[30] J. Lin, H. Hu, N. Gao, J. Ye, Y. Chen, and H. Ou, J. Water Process Eng. 33 (2020) 101010.
[31] H. Hu, H. Zhang, Y. Chen, and H. Ou, Environ. Sci. Pollut. Res. 26 (2019) 24720.
[32] H. Hu, H. Zhang, Y. Chen, Y. Chen, L. Zhuang, and H. Ou, Chem. Eng. J. 368 (2019) 273.
[33] Y. Huang, H. Lin, and Y. Zhang, J. Solid State Chem. 283 (2020) 121150.
[34] A.J. Bard, and L.R. Faulkner, 2001. Fundamentals and applications. Electrochemical methods 2 (482) pp.580-632.